A&A 394, 753–762 (2002)
DOI: 10.1051/0004-6361:20021091


Astronomy & Astrophysics

# Atomic data from the IRON Project

## LI. Electron impact excitation of Fe IX⋆

P. J. Storey[1], C. J. Zeippen[2], and M. Le Dourneuf[3]

[1] Department of Physics and Astronomy, University College London, Gower Street, London WC1E 6BT, UK
[2] LUTH (FRE 2462 associée au CNRS et à l'Université Paris 7), Observatoire de Paris, 92195 Meudon, France
[3] Laboratoire PALMS (UMR 6627 du CNRS – Université de Rennes 1), Équipe SIMPA, Campus de Beaulieu, Université de Rennes 1, 35042 Rennes Cedex, France

Received 29 May 2002 / Accepted 23 July 2002

**Abstract.** We calculate collision strengths and thermally averaged collision strengths for electron excitation between the one hundred and forty energetically lowest levels of $Fe^{8+}$. The scattering target is more elaborate than in any earlier work and large increases are found in the excitation rates among the levels of the $3s^23p^53d$ electron configuration due to resonance series that have not been considered previously. The implications for solar and stellar spectroscopy have been discussed elsewhere (Storey & Zeippen 2001). We correct some errors that were made in generating the figures given in that paper and present corrected versions.

**Key words.** Sun: general – atomic data – Sun: UV radiation

## 1. Dedication

Maryvonne Le Dourneuf had started working on this project when an accident caused her untimely death in November 1997. This paper is dedicated to her memory.

## 2. Introduction

The intensity ratio of the Fe IX $3s^23p^53d\ ^3P^o_2$–$3s^23p^6\ ^1S_0$ magnetic quadrupole transition at 241.7 Å to the $3s^23p^53d\ ^3P^o_1$–$3s^23p^6\ ^1S_0$ intercombination transition at 244.9 Å is of practical interest in solar studies because the two lines lie close in wavelength and are not significantly blended. This makes comparisons of their intensities relatively easy and the ratio is sensitive to electron density over the range $10^9$–$10^{13}$ cm$^{-3}$. Feldman (1992) reviewed the various sets of atomic data available at the time and drew attention to the much larger electron densities derived from flare spectra using the Fe IX $\lambda$241.7/$\lambda$244.9 line intensity ratio compared to those derived from ratios in other ions.

Flower (1977) was the first to compute collision strengths for electron excitation of $Fe^{8+}$ using the distorted wave method while radiative decay rates had been calculated by Garstang (1969) and Flower (1977). Further work was done on the $Fe^{+8}$ atomic model by Haug (1979) who added the effect of cascades from higher energy levels to the original calculation of Feldman et al. (1978). More recently, Fawcett & Mason (1991) reconsidered the atomic data calculations of Flower (1977). Although based on the same computer package composed of DISTWAV (Eissner & Seaton 1972), JAJOM (Saraph 1972, 1978) and SUPERSTRUCTURE (Eissner et al. 1974), this study included an adjustment of Slater parameters (Fawcett & Mason 1989) using a subroutine in the HFR code of Cowan (1981). Also, a lack of consistency in the level indexing in the work of Flower was corrected. Finally, Mandelbaum (1991) provided a new set of atomic data yielded by the code HULLAC (Bar-Shalom et al. 1998), while Liedahl (2000) has used the same code to explore the effect of dramatically increasing the number of states in the Fe IX atomic model. A review of electron excitation data for Fe IX–Fe XIV was also published by Mason (1994) as part of an atomic data assessment study for SOHO.

Liedahl (2000) has shown that the discrepancies between the predicted and observed intensity ratios for the density sensitive lines are significantly reduced if the model atom is increased in size. His model includes electron configurations with valence electron principal quantum numbers $n \leq 4$,

*Send offprint requests to*: P. J. Storey, e-mail: PJS@star.ucl.ac.uk
⋆ Detailed tables of the present data are available in electronic form at the CDS via anonymous ftp to
cdsarc.u-strasbg.fr (ftp 130.79.128.5) or via
http://cdsweb.u-strasbg.fr/cgi-bin/qcat?J/A+A/394/753

**Table 1.** The target configuration basis.

| | |
|---|---|
| $3s^2\ 3p^6$ | $3s^2\ 3p^5\ 3d$ |
| $3s\ 3p^6\ 3d$ | $3s^2\ 3p^5\ 4s$ |
| $3s^2\ 3p^4\ 3d^2$ | |
| $3s^2\ 3p^5\ 4p$ | |
| | |
| $3p^6\ 3d^2$ | $3s\ 3p^5\ 3d^2$ |
| $3s\ 3p^4\ 3d^3$ | $3s^2\ 3p^3\ 3d^3$ |
| | $3p^5\ 3d^3$ |
| | $3s^2\ 3p^5\ 4d$ |

with a total of 1067 levels. He states, however, that the most important contributions probably come from the levels of the $3s^23p^43d^2$ configuration. We note that the collision rates used by Liedahl (2000) do not include resonance effects.

The present work is part of the international collaboration known as the Iron Project (Hummer et al. 1993) whose aim is to make systematic calculations of electron scattering cross-sections and rate coefficients for ions of astronomical interest, using the best available methods. The principal tool of the project is the atomic R-matrix computer code of Berrington et al. (1974, 1978) as extended for use in the Opacity Project (Berrington et al. 1987). These codes have recently been further extended (Hummer et al. 1993 ) so that collision strengths can be calculated at low energies, where some scattering channels are closed, including the effects of intermediate coupling in the target. Previous calculations have always neglected such effects at energies where some channels are closed.

In Sect. 3, we discuss the target used in our Fe IX model. We give details of the electron scattering calculations in Sect. 4 and make a critical comparison with previous work in Sect. 5.

The discrepancies between electron densities derived from lines of Fe IX and other ions of similar ionisation potential in solar spectra are largely removed when line intensities are computed using the results presented here. This is principally due to the inclusion of the $3s^23p^43d^2$ configuration in the scattering process, which profoundly modifies the populations of the levels of the $3s^23p^53d$ configuration, through cascading and through the resonance series that it generates. We return to this latter effect in Sect. 5. For more details of the spectroscopic implications, see Storey & Zeippen (2001) but note that the calculation described here corrects an error that was made in the work of those authors and is also more extensive. We return to these points in Sect. 5.

## 3. The target

A schematic diagram of the term structure of Fe IX is shown in Fig. 1. With the exception of the calculation by Liedahl (2000), all previous work on electron scattering from $Fe^{8+}$ has only included the two energetically lowest electron configurations, comprising seven terms in all. As we shall show below and as has been discussed by Storey & Zeippen (2001), the dipole coupling between the $3s^23p^53d$ and $3s^23p^43d^2$ configurations is very strong and has a profound effect on the rates for electron induced transitions between the levels of the $3s^23p^53d$ configuration. The cross-sections for these processes contain resonance series converging to the terms of the $3s^23p^43d^2$ configuration and it is therefore essential that the target for the scattering problem should include this configuration. Our target, as shown by the dotted line in Fig. 1, includes forty-seven of the forty-nine terms of the $3s^23p^43d^2$ configuration and the two omitted terms have only weak dipole coupling to the lower configuration. The scattering target, constructed from the six energetically lowest electron configurations contains sixty-four terms.

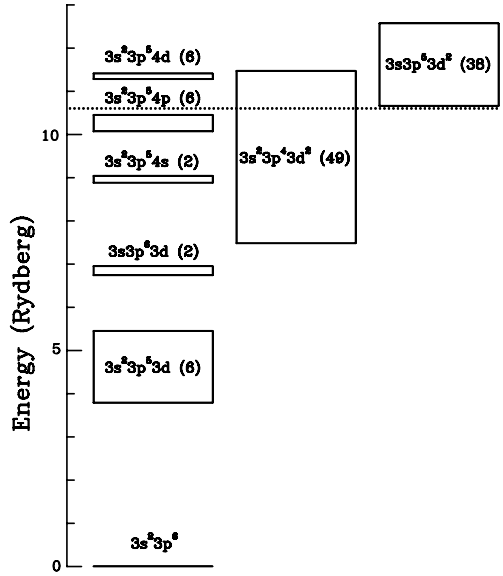


**Fig. 1.** Schematic energy diagram of Fe IX. The numbers in brackets are the numbers of terms in each configuration. The dotted line shows the extent of the present target.

**Table 2.** Potential scaling parameters.

| | | | | | |
|---|---|---|---|---|---|
| 1s | 1.41656 | 2p | 1.06690 | 3d | 1.13662 |
| 2s | 1.11973 | 3p | 1.11736 | 4d | 1.14998 |
| 3s | 1.13742 | 4p | 1.14997 | | |
| 4s | 1.18165 | | | | |

See text for physical significance of the scaling parameters.

The target wavefunctions are expanded in the twelve configuration basis listed in Table 1. The target expansion includes all the electron configurations of the $n = 3$ complex with three or less electrons in a 3d orbital. Also included are the $3s^23p^54s$ and $3s^23p^54p$ configurations which lie energetically within $3s^23p^43d^2$. The lower group of configurations listed in Table 1 are present solely for correlation purposes and only those terms are retained that are present in the actual scattering target. Correlation effects will be discussed further below in the context of the discussion of target oscillator strengths.

The target wavefunctions were constructed using the program SUPERSTRUCTURE, (Eissner et al. 1974; Nussbaumer & Storey 1978), which uses radial wavefunctions calculated in a scaled Thomas-Fermi-Dirac statistical model potential. The scaling parameters were determined by minimizing the sum of the energies of all the target terms, computed in LS-coupling,

**Table 3.** Energies of target terms in Rydberg.

| Term | | Exp.† | Calculated |
|---|---|---|---|
| $3s^23p^6$ | $^1S$ | 0. | 0. |
| $3s^23p^53d$ | $^3P^o$ | 3.7454 | 3.8147 |
| | $^3F^o$ | 3.9083 | 3.9986 |
| | $^1D^o$ | 4.1622 | 4.2474 |
| | $^3D^o$ | 4.1822 | 4.2553 |
| | $^1F^o$ | 4.2449 | 4.3442 |
| | $^1P^o$ | 5.3268 | 5.4794 |
| $3s3p^63d$ | $^3D$ | 6.6344 | 6.7726 |
| $3s3p^63d$ | $^1D$ | 6.8333 | 6.9817 |
| $3s^23p^43d^2$ | $^5S$ | | 7.5085 |
| | $^5D$ | | 7.5669 |
| | $^5F$ | | 7.6620 |
| | $^5G$ | | 7.8280 |
| | $^3P$ | | 7.8549 |
| | $^3F$ | | 7.9531 |
| | $^3G$ | | 8.0031 |
| | $^1D$ | | 8.0988 |
| | $^3F$ | | 8.1239 |
| | $^5D$ | | 8.1671 |
| | $^3D$ | | 8.1914 |
| | $^1S$ | | 8.1958 |
| | $^5P$ | | 8.2265 |
| | $^3H$ | | 8.2416 |
| | $^1F$ | | 8.2870 |
| | $^1G$ | | 8.2963 |
| | $^3D$ | | 8.2972 |
| | $^3G$ | | 8.3397 |
| | $^3P$ | | 8.3441 |
| | $^3H$ | | 8.4271 |
| | $^1P$ | | 8.4820 |
| | $^3F$ | | 8.4901 |
| | $^1I$ | | 8.4967 |
| | $^1G$ | | 8.5735 |
| | $^1D$ | | 8.7151 |
| | $^3D$ | | 8.7564 |
| | $^1H$ | | 8.8153 |
| | $^3P$ | | 8.8215 |
| | $^3F$ | | 8.8642 |

† Corliss & Sugar (1982).

**Table 3.** continued.

| Term | | Exp.† | Calculated |
|---|---|---|---|
| $3s^23p^43d^2$ | $^3G$ | | 9.1089 |
| $3s^23p^54s$ | $^3P^o$ | | 9.1240 |
| $3s^23p^43d^2$ | $^1F$ | | 9.1882 |
| | $^3P$ | | 9.2007 |
| | $^1G$ | | 9.2445 |
| | $^1D$ | | 9.2744 |
| | $^3F$ | | 9.2852 |
| $3s^23p^54s$ | $^1P^o$ | | 9.2908 |
| $3s^23p^43d^2$ | $^3S$ | | 9.3823 |
| | $^3D$ | | 9.4184 |
| | $^3P$ | | 9.4596 |
| | $^1G$ | | 9.4607 |
| | $^1D$ | | 9.5030 |
| | $^1S$ | | 9.6790 |
| | $^3F$ | | 9.7022 |
| | $^1P$ | | 9.7789 |
| | $^1D$ | | 9.7806 |
| | $^3D$ | | 9.8021 |
| | $^3P$ | | 9.8475 |
| $3s^23p^54p$ | $^3S$ | | 9.9050 |
| $3s^23p^43d^2$ | $^1F$ | | 9.9583 |
| $3s^23p^54p$ | $^3D$ | | 10.0492 |
| | $^1P$ | | 10.1744 |
| | $^3P$ | | 10.1866 |
| | $^1D$ | | 10.2369 |
| | $^1S$ | | 10.5897 |

† Corliss & Sugar (1982).

i.e. neglecting all relativistic effects. The resulting scaling parameters are given in Table 2.

The energies of the sixty-four target states are shown in Table 3. The experimental values are taken from Corliss & Sugar (1982). The theoretical energies were calculated including electrostatic interactions plus the one-body mass and Darwin relativistic energy shifts. Fine-structure interactions were neglected. As discussed, for example, by Saraph & Storey (1996), this approximation results in term energies that are significantly better than those obtained from pure LS-coupling. Using this approximation, however, the number of scattering channels remains the same as in pure LS-coupling, avoiding the large increase in computational cost incurred by doing the whole scattering calculation in intermediate coupling.

In Table 4, we give weighted electric dipole oscillator strengths computed in the length and velocity formulations for transitions among the target terms calculated in our target configuration basis. For transitions between the $3s^23p^53d$ and $3s^23p^43d^2$ configurations we give only those for which $gf_L$ is greater than unity. In Table 5 we compare our computed oscillator strengths with those of earlier workers. Almost all prior theoretical work was restricted to transitions from the ground state to the two lowest odd parity configurations, $3s^23p^53d$ and $3s^23p^54s$. The exception is the data computed by Mendoza under the auspices of the Opacity Project and available from the online databank, TOPBASE (Cunto et al. 1993). Apart from this latter work, all earlier computations were made in a very limited, usually two, configuration basis and give a somewhat larger oscillator strength for the $3s^23p^6\,^1S$–$3s^23p^53d\,^1P^o$ resonance transition than we find here. Fawcett & Mason (1991) quote values of $gf$ calculated both ab initio (the first entry in the table) and calculated after empirical adjustment of Slater parameters (the second entry). These authors also give values of both $gf_L$ and $gf_V$, finding a much larger discrepancy than in the present work. The principal cause of these differences is the absence of $3p^n$–$3p^{n-2}3d^2$ correlation. Hence, for the resonance transition the important correlation effects are with the

**Table 4.** Weighted oscillator strengths, $gf$ in the length and velocity formulations for the target.

| Transition | | | | $gf_L$ | $gf_V$ |
|---|---|---|---|---|---|
| $3s^2 3p^6\ ^1S$ | – | $3s^2 3p^5 3d$ | $^1P^o$ | 2.99 | 2.73 |
| | – | $3s^2 3p^5 4s$ | $^1P^o$ | 0.28 | 0.29 |
| $3s^2 3p^5 3d\ ^3P^o$ | – | $3s^2 3p^4 3d^2$ | $^3D$ | 4.70 | 4.84 |
| | – | | $^3S$ | 3.25 | 2.20 |
| | – | | $^3D$ | 1.06 | 0.69 |
| | – | | $^3P$ | 9.57 | 7.13 |
| | – | | $^3D$ | 2.09 | 1.60 |
| $3s^2 3p^5 3d\ ^3F^o$ | – | | $^3D$ | 1.40 | 1.09 |
| | – | | $^3G$ | 15.49 | 15.61 |
| | – | | $^3F$ | 3.38 | 2.69 |
| | – | | $^3D$ | 13.14 | 8.86 |
| | – | | $^3F$ | 16.52 | 12.62 |
| $3s^2 3p^5 3d\ ^1D^o$ | – | | $^1F$ | 2.64 | 2.62 |
| | – | | $^1D$ | 1.78 | 1.82 |
| | – | | $^1D$ | 2.29 | 1.66 |
| | – | | $^1P$ | 2.89 | 1.74 |
| | – | | $^1F$ | 1.35 | 1.22 |
| $3s^2 3p^5 3d\ ^3D^o$ | – | | $^3F$ | 6.38 | 6.12 |
| | – | | $^3F$ | 5.60 | 5.11 |
| | – | | $^3D$ | 13.62 | 10.86 |
| | – | | $^3P$ | 9.05 | 5.84 |
| $3s^2 3p^5 3d\ ^1F^o$ | – | | $^1G$ | 4.82 | 4.94 |
| | – | | $^1D$ | 2.15 | 1.76 |
| | – | | $^1D$ | 2.71 | 1.53 |
| | – | | $^1F$ | 6.01 | 4.74 |

**Table 5.** $gf$ values from the $3s^2 3p^6\ ^1S$ state.

| Authors | Final state | |
|---|---|---|
| | $3s^2 3p^5 3d\ ^1P^o$ | $3s^2 3p^5 4s\ ^1P^o$ |
| Froese (1966) | 3.76 | 0.34 |
| Cowan (1968) | 3.72 | |
| Flower (1977) | 4.1 | |
| Opacity Project† | 3.08 | 0.317 |
| Fawcett & Mason (1991) (length)[1] | 4.13, 3.97 | 0.26, 0.21 |
| Fawcett & Mason (1991) (velocity)[1] | 2.07, 2.14 | 0.26, 0.20 |
| Present (length) | 2.99 | 0.28 |
| Present (velocity) | 2.73 | 0.29 |

† Cunto et al. (1993).

[1] See text for explanation of multiple entries.

$3s^2 3p^4 3d^2$ and $3s^2 3p^3 3d^3$ configurations. The result of including these configurations is to lower $gf_L$ for the resonance transition by about 25% and dramatically reduce the difference between $gf_L$ and $gf_V$ giving confidence the present result is more accurate than any earlier values. There is good agreement with the results available from TOPBASE (Cunto et al. 1993), which is the only other calculation of comparable complexity.

In Table 6 we list the calculated and experimental energies of the 17 levels of the target for which energies are known. The experimental values are from Corliss & Sugar (1982) and the calculations include the one- and two-body fine-structure interactions described by Eissner et al. (1974). The levels are given in the experimental energy order. A list of the calculated energies of all 140 levels of the target is available electronically from the CDS. Table 6 serves as a key to the levels for use in later tabulations of collision strengths and effective collision strengths.

**Table 6.** Energies of target levels in Rydberg.

| Index | Config. | Level | Calculated | Experimental† |
|---|---|---|---|---|
| 1 | $3s^2\ 3p^6$ | $^1S_0$ | 0.00000 | 0.00000 |
| 2 | $3s^2\ 3p^5\ 3d$ | $^3P^o_0$ | 3.76364 | 3.69770 |
| 3 | | $^3P^o_1$ | 3.78883 | 3.72088 |
| 4 | | $^3P^o_2$ | 3.84039 | 3.76967 |
| 5 | | $^3F^o_4$ | 3.97113 | 3.88030 |
| 6 | | $^3F^o_3$ | 4.00201 | 3.91221 |
| 7 | | $^3F^o_2$ | 4.04308 | 3.95329 |
| 8 | | $^3D^o_3$ | 4.25326 | 4.15188 |
| 9 | | $^3D^o_2$ | 4.26847 | 4.16228 |
| 10 | | $^3D^o_1$ | 4.29702 | 4.19748 |
| 11 | | $^1D^o_2$ | 4.31956 | 4.21571 |
| 12 | | $^1F^o_3$ | 4.34420 | 4.24498 |
| 13 | | $^1P^o_1$ | 5.47936 | 5.32683 |
| 14 | $3s\ 3p^6\ 3d$ | $^3D_1$ | 6.75891 | 6.62255 |
| 15 | | $^3D_2$ | 6.76762 | 6.63008 |
| 16 | | $^3D_3$ | 6.78194 | 6.64261 |
| 17 | | $^1D_2$ | 6.98165 | 6.83339 |

† Corliss & Sugar (1982).

## 4. The scattering calculation

The R-matrix method used in this calculation is described fully elsewhere (Hummer et al. 1993 and references therein). As outlined above, we include mass and Darwin relativistic energy shifts, but not the one- and two-body fine-structure interactions. We use an R-matrix boundary radius of 6.41 au, to encompass the most extended target orbital (4d). The expansion of each scattered electron partial wave is over a basis of 24 functions within the R-matrix boundary, and the partial wave expansion extends to a maximum of $l = 15$. The outer region calculation is carried out using the program STGFJ (Hummer et al. 1993), which calculates reactance matrices in LS-coupling and then transforms them into the $Jk$-coupling scheme (Saraph 1972, 1978), including the effects of intermediate coupling between the target terms, using the so-called term-coupling coefficients (TCCs).

Collision strengths in the resonance region are computed at 5108 values of the energy. We do not, therefore attempt to delineate all resonance structures fully. The accuracy of this sampling approach was discussed by Storey et al. (1996). In the region of all channels open, a further 22 points span the energy range from the highest threshold up to 64 Ryd. The number of energies at which collision strengths have been calculated has been approximately doubled since our earlier preliminary report on the spectroscopic implications of the new collision strength calculation (Storey & Zeippen 2001). We return to this point in Sect. 5.

**Table 7.** Comparison of collision strengths above all thresholds.

| $i$ | $j$ | FM91† 15 Ryd | Present 14.4 Ryd | FM91† 45 Ryd | Present 44.8 Ryd |
|---|---|---|---|---|---|
| 1 | 2 | 0.0084 | 0.0093 | 0.0022 | 0.0024 |
| | 3 | 0.0345 | 0.0284 | 0.0080 | 0.0081 |
| | 4 | 0.0554 | 0.0459 | 0.0108 | 0.0117 |
| | 5 | 0.0424 | 0.0351 | 0.0076 | 0.0085 |
| | 6 | 0.0337 | 0.0286 | 0.0085 | 0.0097 |
| | 7 | 0.0227 | 0.0188 | 0.0040 | 0.0045 |
| | 8 | 0.0295 | 0.0316 | 0.0276 | 0.0335 |
| | 9 | 0.0105 | 0.0099 | 0.0013 | 0.0024 |
| | 10 | 0.0168 | 0.0127 | 0.0208 | 0.0145 |
| | 11 | 0.0107 | 0.0091 | 0.0013 | 0.0020 |
| | 12 | 0.0536 | 0.0542 | 0.0654 | 0.0658 |
| | 13 | 5.083 | 4.103 | 8.496 | 6.290 |
| 2 | 3 | 0.0606 | 0.0409 | 0.0074 | 0.0102 |
| | 4 | 0.0300 | 0.0126 | 0.0153 | 0.0085 |
| | 5 | 0.0181 | 0.0123 | 0.0051 | 0.0050 |
| | 6 | 0.0320 | 0.0223 | 0.0043 | 0.0047 |
| | 7 | 0.0611 | 0.0554 | 0.0423 | 0.0496 |
| | 8 | 0.0159 | 0.0102 | 0.0014 | 0.0014 |
| | 9 | 0.0169 | 0.0149 | 0.0094 | 0.0118 |
| | 10 | 0.0138 | 0.0107 | 0.0016 | 0.0021 |
| | 11 | 0.0075 | 0.0146 | 0.0019 | 0.0081 |
| | 12 | 0.0095 | 0.0071 | 0.0013 | 0.0015 |
| | 13 | 0.0052 | 0.0042 | 0.0005 | 0.0007 |
| 3 | 4 | 0.1385 | 0.0876 | 0.0449 | 0.0362 |
| | 5 | 0.0697 | 0.0440 | 0.0147 | 0.0133 |
| | 6 | 0.1334 | 0.1572 | 0.0744 | 0.1344 |
| | 7 | 0.1304 | 0.0724 | 0.0763 | 0.0442 |
| | 8 | 0.0615 | 0.0344 | 0.0120 | 0.0099 |
| | 9 | 0.0275 | 0.0179 | 0.0032 | 0.0045 |
| | 10 | 0.0299 | 0.0331 | 0.0047 | 0.0180 |
| | 11 | 0.0292 | 0.0309 | 0.0037 | 0.0059 |
| | 12 | 0.0497 | 0.0490 | 0.0170 | 0.0231 |
| | 13 | 0.0164 | 0.0134 | 0.0016 | 0.0022 |
| 4 | 5 | 0.2962 | 0.3281 | 0.1600 | 0.2855 |
| | 6 | 0.1735 | 0.0761 | 0.1028 | 0.0461 |
| | 7 | 0.0668 | 0.0372 | 0.0341 | 0.0147 |
| | 8 | 0.1576 | 0.0621 | 0.0435 | 0.0124 |
| | 9 | 0.0586 | 0.0370 | 0.0075 | 0.0074 |
| | 10 | 0.0334 | 0.0357 | 0.0033 | 0.0133 |
| | 11 | 0.0521 | 0.0522 | 0.0051 | 0.0213 |
| | 12 | 0.0855 | 0.0899 | 0.0111 | 0.0200 |
| | 13 | 0.0304 | 0.0244 | 0.0031 | 0.0040 |

† Fawcett & Mason (1991).

For energies above the highest threshold, the collision strengths are corrected for contributions from partial waves of higher angular momentum using the method described by Binello et al. (1998). In brief, for optically allowed transitions contributions from partial waves $l > 15$ are calculated in the Coulomb-Bethe approximation, using oscillator strengths taken from the target calculation including one-body

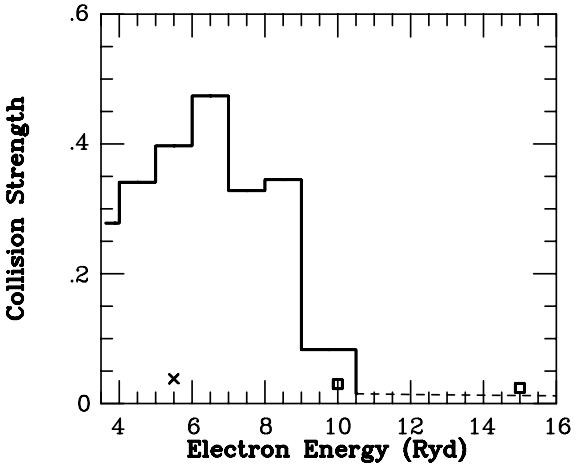


**Fig. 2.** Collision strength for the $3s^23p^53d(^3P^o_0)$–$3s^23p^53d(^3P^o_2)$ transition. Solid line from present results averaged over 1 Ryd intervals in the resonance region. Squares from Fawcett & Mason (1991), cross from Flower (1977).

fine-structure effects (spin-orbit coupling). For the remaining transitions, the contribution from the high partial waves is estimated by assuming that the partial collision strengths are declining geometrically as a function of angular momentum. Once all collision strengths have been corrected for missing angular momenta, they are extrapolated to energies higher than 64 Ryd using techniques and asymptotic expressions discussed by Burgess & Tully (1992). Further details are given in Binello et al. (1998).

## 5. Results and discussion

In Table 7 we compare a selection of our total collision strengths with the work of Fawcett & Mason (1991) The transitions listed include the principal resonance line ($3s^23p^6\ ^1S_0$–$3s^23p^53d\ ^1P^o_1$, indexed 1–13) and the main de-excitation routes from $3s^23p^53d\ ^3P^o_J$ levels to other levels of the $3s^23p^53d$ configuration. At the energies given in Table 7, (15 and 45 Ryd) none of the calculations contain any resonance features. The results of Fawcett & Mason (1991) were obtained using the distorted wave method (Eissner & Seaton 1972) adapted to enable the adjustment of Slater parameters using a subroutine in the HFR code of Cowan (1981). Their target basis contained only the three electron configurations $3s^23p^6$, $3s^23p^53d$, $3s^23p^54s$ and their calculations were made at 10, 15, 30 and 45 Ryd, above all thresholds. The agreement is reasonably good, as one would expect at these relatively high energies, although the value of the collision strength for the ($3s^23p^6\ ^1S_0$–$3s^23p^53d\ ^1P^o_1$) transition obtained by Fawcett & Mason (1991) is larger by 41% at 10 Ryd. This is directly related to the difference found between the oscillator strengths in the two targets (see Table 5 and discussion in Sect. 3).

In Table 8 we compare collision strengths at 5.5 Ryd from an early distorted wave calculation by Flower (1977) with our data. In the present work, the highest target threshold lies at 10.590 Ryd, so there are resonance features present at 5.5 Ryd. The values given in Table 8 were derived from the calculated collision strengths by averaging over the energy

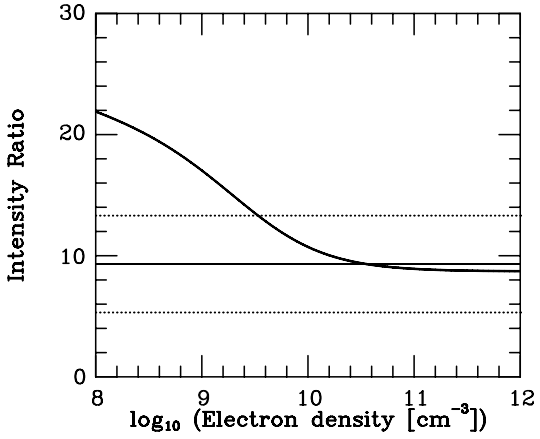


**Fig. 3.** The $\lambda$171.1/ $\lambda$244.9 intensity ratio as function of electron density at $T_e = 9 \times 10^5$ K derived from the present atomic data. The solid horizontal line corresponds to the observed ratio from the SERTS data of Thomas & Neupert (1994). The dotted lines correspond to the errors on the line intensities quoted by Thomas & Neupert (1994).

range 5.0–6.0 Ryd. Once again we find a significantly smaller collision strength for the resonance transition (1–13) but the most striking differences are in the collision strengths from the $3s^2 3p^5 3d\ ^3P^o_J$ levels (2, 3 and 4) to higher levels of the same configuration (5 to 13). These average values are much larger than the results of Flower (1977), by factors ranging from 3.7 to 13.8. These increases are caused by the series of resonances converging on the terms of the $3s^2 3p^4 3d^2$ electron configuration, which have not been included in any earlier work.

In Fig. 2, we show the collision strength for the $3s^2 3p^5 3d(^3P^o_0)$–$3s^2 3p^5 3d(^3P^o_2)$ transition, with the results in the resonance region averaged over 1 Ryd intervals. As described above, there is reasonably good agreement between the present work and that of Fawcett & Mason (1991) in the non-resonant region above 10.6 Ryd, while in the resonant region our results are significantly greater than those of Flower (1977) which do not include resonance effects.

Storey & Zeippen (2001) have discussed the effect of the increased collision strengths on level populations and line intensities. They consider, for example, the density sensitive ratio of the intensities of the $3s^2 3p^5 3d\ ^3P^o_2$–$3s^2 3p^6\ ^1S_0$ magnetic quadrupole transition at 241.7 Å to the $3s^2 3p^5 3d\ ^3P^o_1$–$3s^2 3p^6\ ^1S_0$ intercombination transition at 244.9 Å. Storey & Zeippen (2001) show that the discrepancy discussed by Feldman (1992) betweeen the electron densities derived from this line ratio and those derived from ratios in other comparable ions was largely eliminated by new atomic data similar to that used in the present paper. This is caused in part by the changes in the rates of electron collisional de-excitation of the levels of the $3s^2 3p^5 3d$ electron configuration but also by the population of the same levels through collisional excitation from the ground state to the levels of the $3s^2 3p^4 3d^2$, followed by radiative cascade. This cascade route for the population of the levels of $3s^2 3p^5 3d$ has also been included in the calculation by Liedahl (2000) but he used a much simpler approximation to the scattering process that does not include resonance effects (Bar-Shalom et al. 1998).

**Table 8.** Comparison of collision strengths at 5.5 Ryd.

| $i$ | $j$ | Flower (1977) | Present (average) |
|---|---|---|---|
| 1 | 2 | 0.014 | 0.026 |
| | 3 | 0.041 | 0.077 |
| | 4 | 0.068 | 0.128 |
| | 5 | 0.030 | 0.089 |
| | 6 | 0.043 | 0.126 |
| | 7 | 0.056 | 0.158 |
| | 8 | 0.014 | 0.121 |
| | 9 | 0.013 | 0.033 |
| | 10 | 0.014 | 0.089 |
| | 11 | 0.033 | 0.122 |
| | 12 | 0.049 | 0.180 |
| | 13 | 3.68 | 1.930 |
| 2 | 3 | 0.087 | 0.714 |
| | 4 | 0.038 | 0.397 |
| | 5 | 0.072 | 0.266 |
| | 6 | 0.047 | 0.247 |
| | 7 | 0.029 | 0.239 |
| | 8 | 0.021 | 0.130 |
| | 9 | 0.021 | 0.172 |
| | 10 | 0.012 | 0.166 |
| | 11 | 0.026 | 0.137 |
| | 12 | 0.015 | 0.134 |
| | 13 | 0.009 | 0.042 |
| 3 | 4 | 0.188 | 1.783 |
| | 5 | 0.156 | 0.604 |
| | 6 | 0.172 | 0.859 |
| | 7 | 0.108 | 0.783 |
| | 8 | 0.045 | 0.375 |
| | 9 | 0.046 | 0.425 |
| | 10 | 0.046 | 0.500 |
| | 11 | 0.093 | 0.489 |
| | 12 | 0.070 | 0.474 |
| | 13 | 0.028 | 0.129 |
| 4 | 5 | 0.089 | 0.715 |
| | 6 | 0.213 | 1.101 |
| | 7 | 0.378 | 1.866 |
| | 8 | 0.093 | 0.614 |
| | 9 | 0.054 | 0.415 |
| | 10 | 0.085 | 0.812 |
| | 11 | 0.218 | 1.119 |
| | 12 | 0.136 | 0.991 |
| | 13 | 0.051 | 0.222 |

The results given by Storey & Zeippen (2001) were based on a somewhat coarser energy grid for the tabulation of the collision strengths. The number of energies at which collision strengths were calculated in the region of closed channels was 2145, compared to 5108 in the present paper and the number in the region of all channels open was 13 compared to 22. In the present work, the electron configuration basis used to describe the scattering target has been enlarged compared to

**Table 9.** Thermally averaged collision strengths† among the 13 levels of the $3s^2 3p^6$ and $3s^2 3p^5 3d$ electron configurations.

| $i$ | $j$ | log ($T$[K]) | | | | | | |
|---|---|---|---|---|---|---|---|---|
| | | 5.4 | 5.6 | 5.8 | 6.0 | 6.25 | 6.5 | 7.0 |
| 1 | 2 | 3.123(−2) | 2.712(−2) | 2.301(−2) | 1.906(−2) | 1.454(−2) | 1.064(−2) | 5.214(−3) |
| 1 | 3 | 9.358(−2) | 8.133(−2) | 6.909(−2) | 5.735(−2) | 4.395(−2) | 3.243(−2) | 1.655(−2) |
| 1 | 4 | 1.553(−1) | 1.347(−1) | 1.141(−1) | 9.441(−2) | 7.192(−2) | 5.248(−2) | 2.436(−2) |
| 1 | 5 | 1.480(−1) | 1.284(−1) | 1.073(−1) | 8.693(−2) | 6.420(−2) | 4.547(−2) | 2.020(−2) |
| 1 | 6 | 1.189(−1) | 1.030(−1) | 8.615(−2) | 6.992(−2) | 5.208(−2) | 3.764(−2) | 1.843(−2) |
| 1 | 7 | 8.356(−2) | 7.226(−2) | 6.017(−2) | 4.850(−2) | 3.561(−2) | 2.509(−2) | 1.107(−2) |
| 1 | 8 | 1.215(−1) | 1.033(−1) | 8.564(−2) | 7.030(−2) | 5.582(−2) | 4.650(−2) | 3.832(−2) |
| 1 | 9 | 1.085(−1) | 8.928(−2) | 7.001(−2) | 5.277(−2) | 3.558(−2) | 2.322(−2) | 9.199(−3) |
| 1 | 10 | 2.804(−2) | 2.574(−2) | 2.299(−2) | 2.032(−2) | 1.771(−2) | 1.623(−2) | 1.657(−2) |
| 1 | 11 | 7.701(−2) | 6.471(−2) | 5.171(−2) | 3.967(−2) | 2.727(−2) | 1.806(−2) | 7.245(−3) |
| 1 | 12 | 1.936(−1) | 1.619(−1) | 1.336(−1) | 1.105(−1) | 9.021(−2) | 7.855(−2) | 7.074(−2) |
| 1 | 13 | 3.094( 0) | 3.225( 0) | 3.415( 0) | 3.680( 0) | 4.141( 0) | 4.762( 0) | 6.469( 0) |
| 2 | 3 | 5.757(−1) | 5.303(−1) | 4.492(−1) | 3.535(−1) | 2.427(−1) | 1.573(−1) | 5.989(−2) |
| 2 | 4 | 3.493(−1) | 3.270(−1) | 2.806(−1) | 2.219(−1) | 1.520(−1) | 9.829(−2) | 3.949(−2) |
| 2 | 5 | 1.684(−1) | 1.477(−1) | 1.203(−1) | 9.220(−2) | 6.234(−2) | 4.065(−2) | 1.736(−2) |
| 2 | 6 | 2.002(−1) | 1.753(−1) | 1.438(−1) | 1.118(−1) | 7.709(−2) | 5.079(−2) | 2.000(−2) |
| 2 | 7 | 2.463(−1) | 2.176(−1) | 1.834(−1) | 1.498(−1) | 1.148(−1) | 8.983(−2) | 6.315(−2) |
| 2 | 8 | 1.138(−1) | 9.934(−2) | 8.110(−2) | 6.249(−2) | 4.238(−2) | 2.731(−2) | 1.024(−2) |
| 2 | 9 | 1.172(−1) | 1.016(−1) | 8.314(−2) | 6.507(−2) | 4.639(−2) | 3.310(−2) | 1.896(−2) |
| 2 | 10 | 1.538(−1) | 1.375(−1) | 1.141(−1) | 8.869(−2) | 6.027(−2) | 3.878(−2) | 1.466(−2) |
| 2 | 11 | 1.477(−1) | 1.289(−1) | 1.054(−1) | 8.173(−2) | 5.662(−2) | 3.830(−2) | 1.818(−2) |
| 2 | 12 | 1.046(−1) | 8.955(−2) | 7.169(−2) | 5.430(−2) | 3.624(−2) | 2.316(−2) | 8.698(−3) |
| 2 | 13 | 4.811(−2) | 3.962(−2) | 3.088(−2) | 2.304(−2) | 1.528(−2) | 9.765(−3) | 3.674(−3) |
| 3 | 4 | 1.511( 0) | 1.404( 0) | 1.199( 0) | 9.473(−1) | 6.514(−1) | 4.236(−1) | 1.678(−1) |
| 3 | 5 | 5.842(−1) | 5.093(−1) | 4.136(−1) | 3.167(−1) | 2.139(−1) | 1.386(−1) | 5.553(−2) |
| 3 | 6 | 7.302(−1) | 6.482(−1) | 5.466(−1) | 4.448(−1) | 3.377(−1) | 2.604(−1) | 1.769(−1) |
| 3 | 7 | 5.144(−1) | 4.504(−1) | 3.720(−1) | 2.933(−1) | 2.097(−1) | 1.481(−1) | 7.820(−2) |
| 3 | 8 | 4.055(−1) | 3.541(−1) | 2.888(−1) | 2.224(−1) | 1.512(−1) | 9.857(−2) | 3.961(−2) |
| 3 | 9 | 3.398(−1) | 2.921(−1) | 2.347(−1) | 1.779(−1) | 1.182(−1) | 7.508(−2) | 2.825(−2) |
| 3 | 10 | 3.460(−1) | 3.098(−1) | 2.580(−1) | 2.022(−1) | 1.406(−1) | 9.473(−2) | 4.377(−2) |
| 3 | 11 | 4.518(−1) | 3.962(−1) | 3.241(−1) | 2.492(−1) | 1.681(−1) | 1.077(−1) | 4.027(−2) |
| 3 | 12 | 3.886(−1) | 3.375(−1) | 2.760(−1) | 2.152(−1) | 1.509(−1) | 1.035(−1) | 4.937(−2) |
| 3 | 13 | 1.461(−1) | 1.205(−1) | 9.402(−2) | 7.031(−2) | 4.677(−2) | 2.999(−2) | 1.138(−2) |

that of Storey & Zeippen (2001) by including the configurations $3s^2 3p^5 4p$ and $3s^2 3p^5 4d$. The first of these configurations, which was also included in the target, makes a significant contribution to the cascade effects discussed above. In addition, the computer codes used by Storey & Zeippen (2001) to compute the thermally averaged collision strengths were found to contain an error that caused the collision rates to high lying states to be incorrect. As a result, the comparison of theoretical line intensity ratios given in Storey & Zeippen (2001) is not accurate in detail although the broad conclusions are not affected. We therefore repeat the discussion of the intensity ratios below.

In Table 9, the final thermally averaged collision strengths between the levels of the $3s^2 3p^6$ and the $3s^2 3p^5 3d$ electron configurations are given as a function of electron temperature. The complete set of effective collision strengths among all of the 140 levels of the target are available in electronic form from the CDS. Note that any model of the level populations of the $Fe^{8+}$ must include the full set of 140 levels due to the contributions of cascading from the higher levels.

### 5.1. The $\lambda$171.1/$\lambda$244.9 line intensity ratio

The $\lambda$171.1 line is a strong optically allowed transition from the $3s^2 3p^5 3d\ ^1P^o$ state, populated almost entirely by electron impact excitation from the $3s^2 3p^6\ ^1S_0$ ground state. The $\lambda$171.1/$\lambda$244.9 line intensity ratio demonstrates a weak density dependence, which is shown in Fig. 3 over the density range $10^8$–$10^{12}$ cm$^{-3}$. In this figure as well as in all subsequent quoted theoretical ratios an electron temperature of $9 \times 10^5$ K has been assumed.

From the SERTS data of Thomas & Neupert (1994), we find that the observed ratio is 9.3 ± 4.0, corresponding to a theoretical minimum density of $\log(N_e) = 9.5$, although plainly the error bars are very large. The quiet Sun spectrum of Malinovsky & Heroux (1973) shows both the $\lambda$171.1

**Table 9.** continued.

| $i$ | $j$ | log ($T$[K]) | | | | | | |
|---|---|---|---|---|---|---|---|---|
| | | 5.4 | 5.6 | 5.8 | 6.0 | 6.25 | 6.5 | 7.0 |
| 4 | 5 | 1.590( 0) | 1.406( 0) | 1.181( 0) | 9.570(−1) | 7.236(−1) | 5.561(−1) | 3.758(−1) |
| 4 | 6 | 8.588(−1) | 7.468(−1) | 6.076(−1) | 4.685(−1) | 3.226(−1) | 2.173(−1) | 1.036(−1) |
| 4 | 7 | 5.221(−1) | 4.562(−1) | 3.709(−1) | 2.841(−1) | 1.920(−1) | 1.250(−1) | 5.237(−2) |
| 4 | 8 | 9.540(−1) | 8.387(−1) | 6.866(−1) | 5.279(−1) | 3.556(−1) | 2.276(−1) | 8.491(−2) |
| 4 | 9 | 5.623(−1) | 4.801(−1) | 3.853(−1) | 2.927(−1) | 1.956(−1) | 1.249(−1) | 4.700(−2) |
| 4 | 10 | 3.210(−1) | 2.871(−1) | 2.393(−1) | 1.879(−1) | 1.309(−1) | 8.767(−2) | 3.813(−2) |
| 4 | 11 | 6.557(−1) | 5.803(−1) | 4.781(−1) | 3.704(−1) | 2.532(−1) | 1.664(−1) | 7.001(−2) |
| 4 | 12 | 8.484(−1) | 7.393(−1) | 6.051(−1) | 4.693(−1) | 3.224(−1) | 2.118(−1) | 8.390(−2) |
| 4 | 13 | 2.505(−1) | 2.067(−1) | 1.617(−1) | 1.212(−1) | 8.094(−2) | 5.209(−2) | 1.984(−2) |
| 5 | 6 | 3.405( 0) | 3.116( 0) | 2.633( 0) | 2.074( 0) | 1.429( 0) | 9.344(−1) | 3.722(−1) |
| 5 | 7 | 1.154( 0) | 1.056( 0) | 8.888(−1) | 6.936(−1) | 4.701(−1) | 3.007(−1) | 1.132(−1) |
| 5 | 8 | 2.665( 0) | 2.434( 0) | 2.096( 0) | 1.732( 0) | 1.337( 0) | 1.046( 0) | 7.351(−1) |
| 5 | 9 | 9.002(−1) | 7.949(−1) | 6.556(−1) | 5.128(−1) | 3.603(−1) | 2.483(−1) | 1.239(−1) |
| 5 | 10 | 3.579(−1) | 3.198(−1) | 2.631(−1) | 2.024(−1) | 1.363(−1) | 8.741(−2) | 3.380(−2) |
| 5 | 11 | 1.013( 0) | 9.057(−1) | 7.551(−1) | 5.968(−1) | 4.250(−1) | 2.973(−1) | 1.537(−1) |
| 5 | 12 | 1.830( 0) | 1.627( 0) | 1.356( 0) | 1.078( 0) | 7.849(−1) | 5.752(−1) | 3.545(−1) |
| 5 | 13 | 3.091(−1) | 2.609(−1) | 2.091(−1) | 1.608(−1) | 1.109(−1) | 7.361(−2) | 2.945(−2) |
| 6 | 7 | 2.528( 0) | 2.301( 0) | 1.940( 0) | 1.527( 0) | 1.055( 0) | 6.934(−1) | 2.813(−1) |
| 6 | 8 | 1.457( 0) | 1.276( 0) | 1.052( 0) | 8.244(−1) | 5.821(−1) | 4.055(−1) | 2.146(−1) |
| 6 | 9 | 1.257( 0) | 1.147( 0) | 9.882(−1) | 8.176(−1) | 6.310(−1) | 4.924(−1) | 3.379(−1) |
| 6 | 10 | 7.450(−1) | 6.774(−1) | 5.779(−1) | 4.720(−1) | 3.577(−1) | 2.750(−1) | 1.875(−1) |
| 6 | 11 | 1.199( 0) | 1.093( 0) | 9.367(−1) | 7.675(−1) | 5.829(−1) | 4.478(−1) | 3.030(−1) |
| 6 | 12 | 1.340( 0) | 1.200( 0) | 9.936(−1) | 7.697(−1) | 5.240(−1) | 3.426(−1) | 1.451(−1) |
| 6 | 13 | 2.601(−1) | 2.197(−1) | 1.764(−1) | 1.364(−1) | 9.537(−2) | 6.492(−2) | 2.890(−2) |
| 7 | 8 | 6.219(−1) | 5.564(−1) | 4.609(−1) | 3.590(−1) | 2.481(−1) | 1.664(−1) | 7.746(−2) |
| 7 | 9 | 8.942(−1) | 8.153(−1) | 6.867(−1) | 5.403(−1) | 3.737(−1) | 2.468(−1) | 1.026(−1) |
| 7 | 10 | 1.155( 0) | 1.076( 0) | 9.508(−1) | 8.136(−1) | 6.644(−1) | 5.571(−1) | 4.469(−1) |
| 7 | 11 | 8.947(−1) | 8.158(−1) | 6.987(−1) | 5.724(−1) | 4.345(−1) | 3.335(−1) | 2.253(−1) |
| 7 | 12 | 8.229(−1) | 7.301(−1) | 6.012(−1) | 4.649(−1) | 3.157(−1) | 2.039(−1) | 7.802(−2) |
| 7 | 13 | 1.886(−1) | 1.586(−1) | 1.266(−1) | 9.692(−2) | 6.650(−2) | 4.396(−2) | 1.757(−2) |
| 8 | 9 | 1.333( 0) | 1.239( 0) | 1.053( 0) | 8.300(−1) | 5.706(−1) | 3.729(−1) | 1.532(−1) |
| 8 | 10 | 6.207(−1) | 5.895(−1) | 5.082(−1) | 4.035(−1) | 2.788(−1) | 1.830(−1) | 7.750(−2) |
| 8 | 11 | 1.827( 0) | 1.744( 0) | 1.546( 0) | 1.296( 0) | 9.974(−1) | 7.657(−1) | 5.026(−1) |
| 8 | 12 | 3.336( 0) | 3.152( 0) | 2.711( 0) | 2.151( 0) | 1.488( 0) | 9.804(−1) | 4.224(−1) |
| 8 | 13 | 3.900(−1) | 3.235(−1) | 2.563(−1) | 1.972(−1) | 1.401(−1) | 1.011(−1) | 6.008(−2) |
| 9 | 10 | 6.497(−1) | 6.177(−1) | 5.372(−1) | 4.323(−1) | 3.044(−1) | 2.025(−1) | 8.242(−2) |
| 9 | 11 | 1.528( 0) | 1.459( 0) | 1.260( 0) | 9.968(−1) | 6.775(−1) | 4.310(−1) | 1.600(−1) |
| 9 | 12 | 1.961( 0) | 1.826( 0) | 1.593( 0) | 1.324( 0) | 1.019( 0) | 7.896(−1) | 5.400(−1) |
| 9 | 13 | 4.032(−1) | 3.274(−1) | 2.509(−1) | 1.834(−1) | 1.184(−1) | 7.415(−2) | 2.844(−2) |
| 10 | 11 | 1.070( 0) | 1.019( 0) | 8.948(−1) | 7.325(−1) | 5.352(−1) | 3.793(−1) | 1.985(−1) |
| 10 | 12 | 4.898(−1) | 4.525(−1) | 3.838(−1) | 3.030(−1) | 2.092(−1) | 1.366(−1) | 5.319(−2) |
| 10 | 13 | 1.072(−1) | 8.813(−2) | 6.852(−2) | 5.092(−2) | 3.349(−2) | 2.117(−2) | 7.785(−3) |
| 11 | 12 | 1.397( 0) | 1.306( 0) | 1.125( 0) | 9.064(−1) | 6.518(−1) | 4.576(−1) | 2.409(−1) |
| 11 | 13 | 3.028(−1) | 2.465(−1) | 1.894(−1) | 1.391(−1) | 9.033(−2) | 5.700(−2) | 2.234(−2) |
| 12 | 13 | 5.545(−1) | 4.642(−1) | 3.730(−1) | 2.931(−1) | 2.165(−1) | 1.647(−1) | 1.111(−1) |

† In this table, 3.123(−2) denotes $3.123 \times 10^{-2}$.

and $\lambda$244.9 lines, and although those authors did not give a measured intensity for the $\lambda$244.9 line, from their spectra one can estimate that the ratio is approximately 10. These observations are in pronounced disagreement with the theoretical value of 33 quoted by Young et al. (1998) based on the earlier atomic data as incorporated in the CHIANTI database. The agreement between observation and theory is considerably better using the present atomic data. The very low theoretical values of this

ratio reported by Storey & Zeippen (2001) at low densities were incorrect.

### 5.2. The λ241.7/λ244.9 line intensity ratio

Theoretical values of this ratio as a function of electron density have been given by Feldman (1992). In Fig. 4, we reproduce two of the curves given by Feldman, derived from the atomic data of Flower (1977) and Fawcett & Mason (1991), in addition to the curve obtained from the model of Liedahl (2000) and using the present data. There is reasonable agreement between all three theoretical curves at the lower electron densities, but with the new atomic data, the ratio falls more rapidly with increasing electron density, with the current value being smaller by a factor of 7.9 than that obtained by Feldman (1992) from the data of Fawcett & Mason at $N_e = 10^{11}$ cm$^{-3}$ and a factor of 2.4 smaller than given by Liedahl (2000) at the same density.

We can compare these new theoretical predictions with various observations. From the quiet Sun spectra of Malinovsky & Heroux (1973), we can estimate the ratio to be 2, consistent with $\log(N_e) = 8.85$ (not shown in Fig. 4). From the SERTS data of Thomas & Neupert (1994), we find a ratio of $1.20 \pm 0.56$ implying $\log(N_e) = 9.4 \pm 0.4$ compared to $\log(N_e) = 10.1$ found by Young et al. (1998) using the data incorporated in CHIANTI. The new value of $N_e$ is in significantly better agreement with densities deduced from diagnostic ratios in other Fe ions from the same SERTS data (e.g. Brickhouse et al. 1995). The λ241.7 and λ244.9 lines were also observed and measured in the Skylab data reported by Dere et al. (1979). They found a value of 0.46 for the λ241.7/λ244.9 line intensity ratio in the 1973 Dec. 17 flare, which corresponds to an electron density of $10^{10.0}$ cm$^{-3}$ with the new atomic data, while Dere et al. (1979) deduced a density five times larger using the atomic data available at the time (Flower 1977). The densities deduced from the present atomic data are minor corrections (within 10%) to those reported earlier by Storey & Zeippen (2001) except for those obtained from the quiet Sun data of Malinovsky & Heroux (1973) which are about a factor of two larger.

### 5.3. The λ217.1/λ244.9 line intensity ratio

In their description of the SERTS data, Thomas & Neupert (1994) report a measurement of the λ217.1 line originating from the $3p^5 3d\ ^3D^o_1$ level. In our present atomic model, this line shows a weak density sensitivity when compared to the λ244.9 intercombination line, with the λ217.1/λ244.9 intensity ratio varying from 0.57 to 0.84 between $\log(N_e) = 9$ and $\log(N_e) = 12$. These results are somewhat lower than those quoted by Storey & Zeippen (2001). The observed ratio from the SERTS data is $0.43 \pm 0.24$ while our theoretical value at the density deduced from the SERTS line ratios discussed above ($\log(N_e) = 9.5$) is 0.63. Storey & Zeippen (2001) concluded that in view of the good agreement now obtained for the two line ratios discussed above, the most likely explanation for this discrepancy is the uncertainty in the flux of λ217.1 which was measured in second order at λ434.2 in the SERTS spectrum. It has been proposed (Brickhouse et al. 1995; Young et al. 1998) that the intensities of lines measured in second order are about a factor of two too weak compared to first order lines. The current results tend to confirm this general conclusion although the actual value of the factor appears to be less than two.

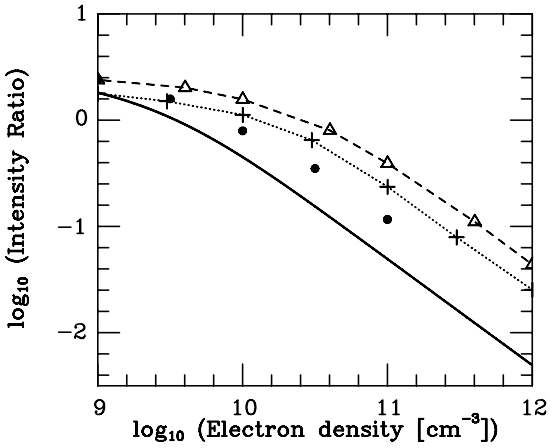


**Fig. 4.** The λ241.7/λ244.9 intensity ratio as function of electron density at $T_e = 9 \times 10^5$ K. The solid line is derived from the present atomic data. Crosses and triangles are values of the ratio taken from Feldman (1992), which were derived from the atomic data of Flower (1977) and Fawcett & Mason (1991), respectively. The filled circles are taken from the 1067-state model of Liedahl (2000). Note that using the present data, the critical electron densities for collisional de-excitation of the $3p^5 3d\ ^3P^o_2$ and $^3P^o_1$ levels are approximately $3 \times 10^9$ and $6 \times 10^{16}$ cm$^{-3}$ respectively.

## 6. Summary

The atomic calculations presented here are a significant advance over previous work. In particular, we have shown that previously unaccounted for resonances converging on the $3s^2 3p^4 3d^2$ electron configuration substantially increase the thermally averaged collision strengths for the transitions among the metastable levels of the $3s^2 3p^5 3d$ configuration. The collisional excitation rate for the principal resonance transition is significantly smaller than in any previous calculation due to the improvement in the target wavefunctions. An error in the earlier work of Storey & Zeippen (2001) has been corrected and the spectroscopic significance of the resulting line ratios has been discussed. Only the λ171.1/λ244.9 line intensity ratio reported here is significantly different from the preliminary results of Storey & Zeippen (2001).

*Acknowledgements.* We acknowledge financial support for the IRON Project from PPARC. The present collaboration benefited from visits to Meudon by PJS between 1998 and 2002, with support provided by the Observatoire de Paris and by the Université Paris 7. The hospitality of the Observatoire de Paris was much appreciated.

## References

Bar-Shalom, A., Klapisch, M., Goldstein, W. H., & Oreg, J. 1998, The Hullac code for atomic physics, unpublished

Berrington, K. A., Burke, P. G., Butler, K., et al. 1987, J. Phys. B, 20, 6379

Berrington, K. A., Burke, P. G., Chang, J. J., et al. 1974, Comput. Phys. Commun., 8, 149
Berrington, K. A., Burke, P. G., Le Dourneuf, M., et al. 1978, Comput. Phys. Commun., 14, 367
Binello, A. M., Mason, H. E., & Storey, P. J. 1998, A&AS, 127, 545
Brickhouse, N. S., Raymond, J. C., & Smith B. W. 1995, ApJS, 97, 551
Burgess, A., & Tully, J. 1992, A&A, 254, 436
Corliss, C., & Sugar, J. 1982, J. Phys. Chem. Ref. Data, 11, 200
Cowan, R. D. 1968, J. Opt. Soc. Am., 58, 924
Cowan, R. D. 1981, The Theory of Atomic Spectra (Univ. of California Press, Los Angeles)
Cunto, W., Mendoza, C., Ochsenbein, F., & Zeippen, C. J. 1993, A&A, 275, L5
Dere, K. P., Mason, H. E., Widing, K. G., & Bhatia, A. K. 1979, ApJS, 40, 341
Eissner, W., Jones, M., & Nussbaumer, H. 1974, Comput. Phys. Commun., 8, 270
Eissner, W., & Seaton, M. J. 1972, J. Phys. B, 5, 2187
Fawcett, B. C., & Mason, H. E. 1989, At. Data Nucl. Data Tables, 43, 245
Fawcett, B. C., & Mason, H. E. 1991, At. Data Nucl. Data Tables, 47, 17
Feldman, U. 1992, ApJ, 385, 758
Feldman, U., Doschek, G. A., & Widing, K. G. 1978, ApJ, 219, 304
Flower, D. R. 1977, A&A, 56, 451
Froese, C. 1966, Bull. Astr. Inst. Neth. 19, 86
Garstang, R. H. 1969, Publ. Astr. Soc. Pac., 81, 488
Haug, E. 1979, ApJ, 228, 903
Hummer, D. G., Berrington, K. A., Eissner, W., et al. 1993, A&A, 279, 298
Liedahl, D. A. 2000, Atomic Data Needs for X-ray Astronomy, ed. M. A. Bautista, T. R. Kallman, & A. K. Pradhan, http://heasarc.gsfc.nasa.gov/docs/heasarc/atomic
Malinovsky, M., & Heroux, L. 1973, ApJ, 181, 1009
Mandelbaum, P. 1991, private communication to Feldman (1992)
Mason, H. E. 1994, At. Data Nucl. Data Tables, 57, 305
Nussbaumer, H., & Storey, P. J. 1978, A&A, 64, 139
Saraph, H. E. 1972, Comput. Phys. Commun., 3, 256
Saraph, H. E. 1978, Comput. Phys. Commun., 15, 247
Saraph, H. E., & Storey, P. J. 1996, A&A, 115, 151
Storey, P. J., Mason, H. E., & Saraph, H. E. 1996, A&A, 309, 677
Storey, P. J., & Zeippen, C. J. 2001, MNRAS, 324, L7
Thomas, R. J., & Neupert, W. M. 1994, ApJS, 91, 461
Young, P. R., Landi, E., & Thomas, R. J. 1998, A&A, 329, 291